Improvement of the thermoplastic formability of $Zr_{65}Cu_{17.5}Ni_{10}Al_{7.5}$ bulk metallic glass by minor addition of Erbium

Q. Hu[a,c], X.R. Zeng[a,d,一], M.W. Fu[b,*], S.S. Chen[a]

[a] Shenzhen Key Laboratory of Special Functional Materials, College of Materials Science and Engineering, and Key Laboratory of Optoelectronic Devices and Systems of Ministry of Education and Guangdong Province, College of Optoelectronic Engineering, Shenzhen University, Shenzhen 518060, China

[b] Department of Mechanical Engineering, The Hong Kong Polytechnic University, Hung Hom, Kowloon, Hong Kong, China

[c] Institute of Applied Physics, Jiangxi Academy of Sciences, Nanchang 330029, China

[d] JANUS Precision Components Co., LTD., Dongguan 523000, China

Abstract

The softness of $Zr_{65}Cu_{17.5}Ni_{10}Al_{7.5}$ bulk metallic glass (BMG) in the super-cooled liquid range (SCLR) is obviously improved by minor addition of 2 percent Er, which makes $(Zr_{65}Cu_{17.5}Ni_{10}Al_{7.5})_{98}Er_2$ (Zr65Er2) to be a very formable Be-free Zr-based BMG. It is found the lower glass transition temperature of Zr65Er2 has an important contribution to the improvement of formability, which is contrary to the general understanding that the larger fragility and wider super-cooled liquid region (SCLR) are the major reasons for better thermoplastic formability. This finding is well explained by using the linear simplification of the SCLR in Angell plot. Zr65Er2 also has lower crystallization temperature and melting temperature, which is believed to be related to the formation of short-range ordering with lower transition energy rather than the composition shift to near eutectic. The above results help understand the effect of minor addition of rare-earth to the formability of Zr-based bulk

一 Corresponding author. Tel.: +86 755 26557459
E-mail address: zengxier@szu.edu.cn (X.R. Zeng)
∗ Corresponding author. Tel.: +852 27665527
E-mail address: mmmwfu@polyu.edu.hk (M.W. Fu)

metallic glasses.

1. Introduction

Similar to many other glasses, bulk metallic glasses (BMGs) are hard at room temperature, but viscous at above glass transition temperature T_g. The former characteristic ensures the outstanding mechanical properties of the materials in practical use, while the latter can be employed to fabricate complex components by using thermoplastical forming process [1-13]. In forming of BMG components, a paramount factor to be considered is the thermoplastic formability, which determines whether a qualified component with complex geometries and fully amorphous structure can be successfully formed. Theoretically, formability is determined by viscosity and crystallization incubation time [14, 15]. But it is not convenient to measure these two temperature-sensitive parameters accurately at the temperature in super-cooled liquid range (SCLR) [16]. The deformation in the whole SCLR with constant heating is thus usually used to compare the formability of different BMGs. The deformation amount, on the other hand, can be represented by the diameter [16, 17] or the length shrinkage[18, 19] of the pressed bulk samples, and the height[20] of the blow formed membrane. In general, large fragility index m and broad the SCLR width ΔT_x are considered to be the most important factors for better formability [16], where m is defined as the rate of viscosity drop at T_g in Angell plot ($\log_{10} \eta \sim T_g/T$) [21], i.e. $m = (d(\log_{10} \eta)/d(T_g/T))_{T=T_g}$. m and ΔT_x determine how quick and how long the viscosity can decrease with the increase of temperature in SCLR, respectively. However, with the advance of research on formability, it is

found that only ΔT_x and m are not sufficient enough to explain the different formability of different BMGs. Similar to the research methodology used in study of glass-forming ability [22, 23], some temperature based parameters are proposed for evaluation of the formability of BMGs [16, 18, 24]. It is found that T_g has a clear effect on the formabilities of a series of BMGs [16, 18], i.e. the BMGs with low T_g usually have good formability. This regularity, although it happens in some BMG cases [25-27], has not yet been received enough attention so far and thus deserves further investigation and in-depth study.

Among a dozen of BMG systems developed in the last decades, Pt-, Au- and Pd-based BMGs have the best formability, followed by Zr-, Mg- and rare-earth based BMGs [16-19, 28-30]. Taking into account the formability, mechanical and corrosion-resistance properties, cost and environment factors, Be-free Zr-based BMGs are the most potential candidate for wide applications and mass production of BMG components. In Be-free Zr-based BMG systems, $Zr_{65}Cu_{17.5}Ni_{10}Al_{7.5}$ (Zr65) has very good formability [18, 31, 32]. It is well known the minor addition of rare-earth can improve the glass-forming ability of Zr-based BMGs by scavenging the oxygen impurity of the melt and increasing the thermal stability of SCLR [33, 34]. Previous arts show the minor addition of several heavy rare-earth elements improves the thermoplastic formability of Zr65 [19], especially for Er. In this paper, the fact that the formability of $(Zr_{65}Cu_{17.5}Ni_{10}Al_{7.5})_{98}Er_2$ (Zr65Er2) is better than that of Zr65 is analysed in depth and it is found that it is caused not only by its larger ΔT_x but also by its lower T_g.

2. Experimental procedure

BMG rods with the diameter of 2 mm were fabricated by copper mould casting and their

amorphous state was confirmed by x-ray diffraction. The glass transition, crystallization and melting behaviors were investigated by differential scanning calorimetry tests (Perkin Elmer DSC7, Setaram SETSYS Evolution 1750), and the softness in SCLR was measured by thermo-mechanical analysis test (Perkin Elmer TMA7).

3. Results

Fig. 1 shows the TMA results of Zr65 and Zr65Er2. The softness in the SCLR determined by TMA test is proven to reflect the thermoplastic formability effectively and conveniently [18]. Addition of a small amount of Er results in the increase of softness by 43%, which makes Zr65Er2 to have the best thermoplastic formability in Be-free Zr-based BMGs family [18, 19]. Based on the Stefan equation [17, 35], the viscosity η with the geometrical correction of viscous flow is calculated as

$$\eta = 2 \times (\sigma / 3\dot{\varepsilon}) / (1 + d_0^2 / 8l_0^2 (1 + \varepsilon_n)^2) \tag{1},$$

where σ, $\dot{\varepsilon}$, d_0, l_0 and ε_n are true stress, strain rate, initial diameter, initial length and nominal strain, respectively. Stress σ is calculated by $\sigma = (F / S_0) \times (l / l_0)$, where F and S_0 are the applied load and the initial cross-sectional area, respectively. Strain ε_n is calculated as $\varepsilon_n = (l_0 - l) / l_0$. Fig. 2 shows the logarithm values of viscosity derived from the TMA results. When the temperature approaches T_g, the relaxation time is about in the magnitude of several minutes [36]. At the heating rate of 20 K/min, the change of viscosity is slower than the change of temperature, resulting in the step-like traces in 600-630 K shown in Fig. 2. In addition, due to the slow relaxation, the measured viscosity in 600-630 K is about an order of magnitude lower than 10^{12} Pa·s that is deemed as the equilibrium viscosity at glass transition

[21]. The measured viscosity changes continuously and smoothly with the elevated temperature above 640 K due to the faster relaxation in SCLR. Until about 720 K, the viscosity increases suddenly for crystallization. For the two BMGs, except the different fluctuation in 640-680 K, the most difference shown in Fig. 2 is that the Zr65Er2 has a lower viscosity before crystallization. As shown in Fig. 2, $\Delta(Log_{10}\eta)$ is used to quantify the total viscosity drop before crystallization, which is also an indicator of the thermoplastic formability [17].
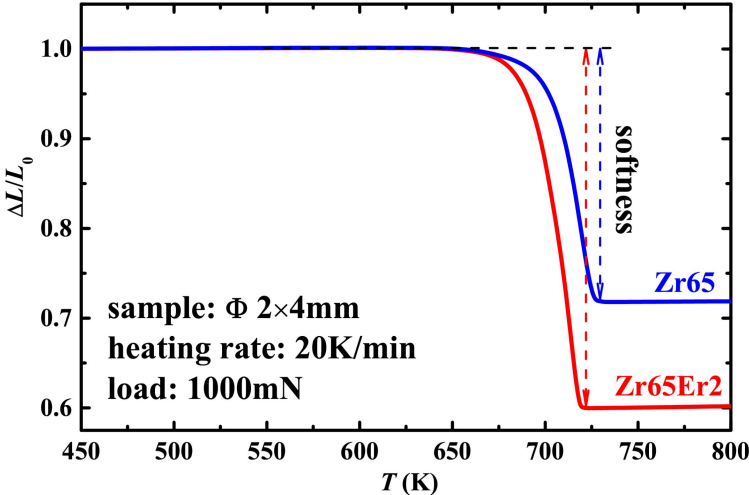
Fig. 1 TMA traces of Zr65 and Zr65Er2 BMGs.
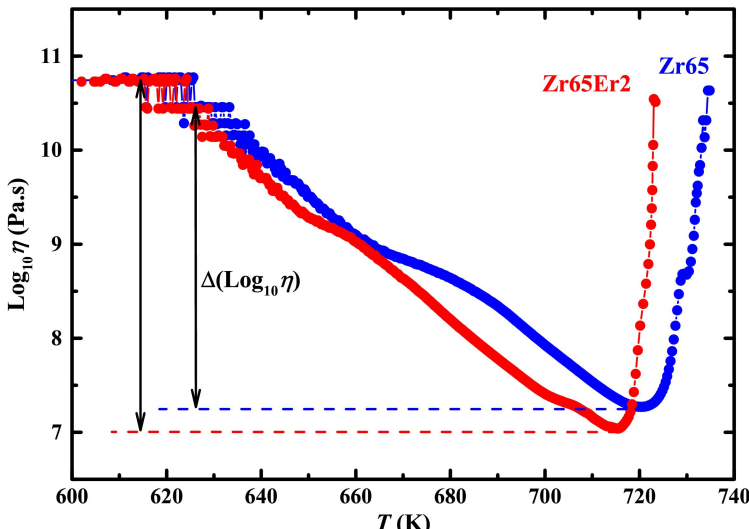
Fig. 2 Viscosities of Zr65 and Zr65Er2 BMGs.
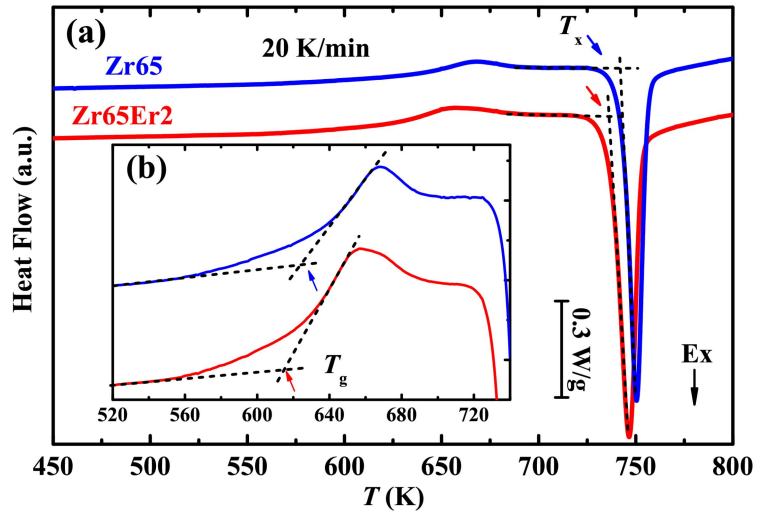
Fig. 3 Glass transition and crystallization of Zr65 and Zr65Er2 BMGs.
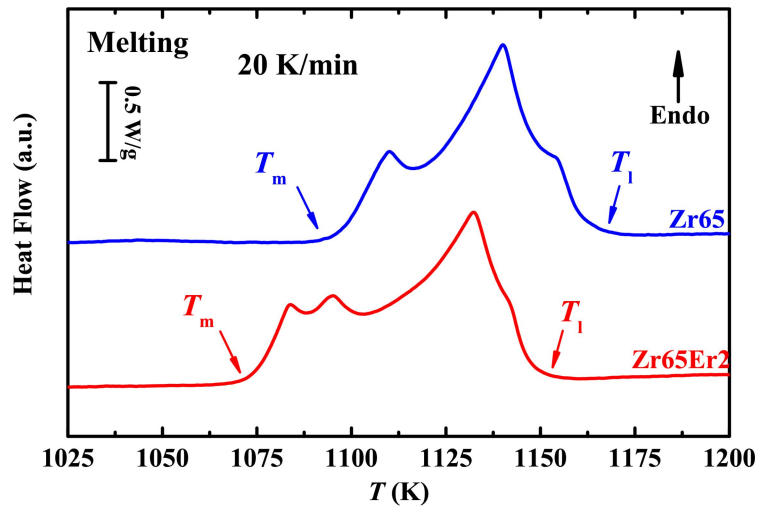
Fig. 4 Melting traces of Zr65 and Zr65Er2 BMGs.
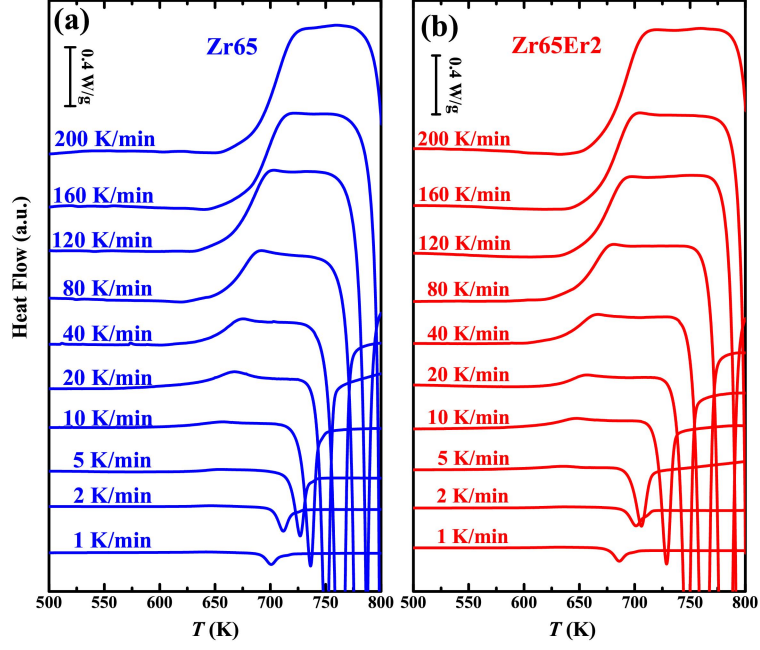
Fig. 5 DSC traces of Zr65 and Zr65Er2 BMGs at different heating rate.
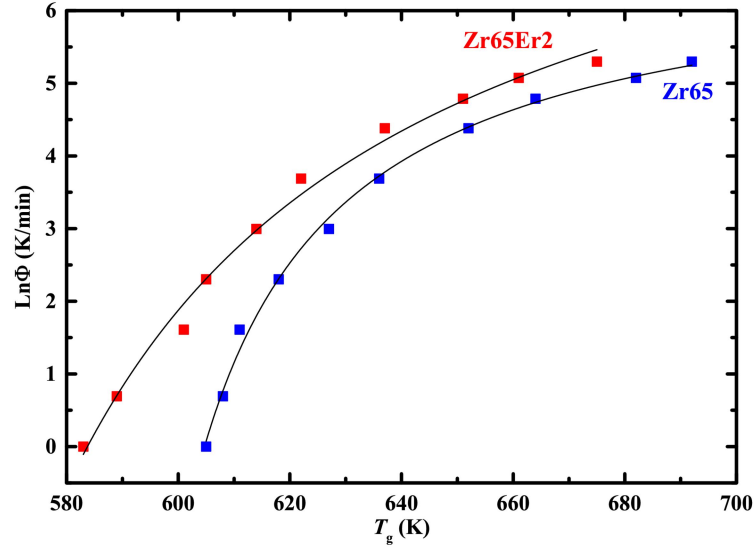
Fig. 6 The fitted relationship of T_g and $\text{Ln}\,\Phi$ by VF equation.

Table 1 Thermal properties of Zr65 and Zr65Er2 BMGs.

BMGs	T_g (K)	T_x (K)	ΔT_x (K)	T_m (K)	T_m (K)	D^*	T_g^0 (K)	m	softness	$\Delta(\text{Log}_{10}\eta)$
Zr65	627	741	114	1097	1167	0.304	579	20.7	0.28	3.5
Zr65Er2	614	735	121	1074	1152	1.161	524	20.1	0.40	3.7

The onset glass transition temperature T_g, crystallization temperature T_x, onset melting temperature T_m and offset temperature T_l are shown in Figs. 3 and 4, respectively. With addition of Er, T_g and T_x decrease 13 K and 6 K respectively, resulting in 7 K increase in ΔT_x ($\Delta T_x = T_x - T_g$). Compared with the obviously improvement in formability, the increase in ΔT_x is relatively small. The other factor, i.e. the fragility index m thus need to be investigated to explain the better formability of Zr65Er2. Since the viscosity relaxation and the glass transition measured by calorimetric methods occur on the same time scale, the heating rate Φ dependent glass transition can be used as a convenient way to determine the fragility of the glasses [37]. The relationship of T_g and $\mathrm{Ln}\Phi$ in case of not fast Φ is usually linearly and can be expressed by Lasocka's relation, although with a fast heating rate above 80 K/min, the relationship is usually nonlinear and fitted more well by the Vogel–Fulcher (VF) equation in the following [38-41]

$$\mathrm{Ln}\Phi = \mathrm{Ln}B - D^* \times T_g / (T_g - T_g^0) \tag{2},$$

where B is a constant, D^* is the strength parameter which can be used to describe how closely the relationship obeys the Arrhenius law [21] and T_g^0 is the VF temperature. From the VF fit, m at a particular T_g can be estimated as

$$m = (D^* / \mathrm{Ln}10) \times (T_g^0 / T_g) / (1 - T_g^0 / T_g)^2 \tag{3}.$$

The glass transition behaviors of Zr65 and Zr65Er2 at different heating rate Φ are shown in Fig. 5. The fitted curve of Zr65Er2 shown in Fig. 6 is less curving and located in the lower temperature range, indicating it has a larger D^* and lower T_g^0 than those of Zr65. The fitted results and the m at the heating rate of 20 K/min are listed in Table 1. It is worth pointing out

that both two BMGs have quite small m when compared with other BMG systems [42-47]. The quite small m is also reported in a group of Zr-Cu-Ni-Al BMGs[48] and maybe due to the network microstructures of this BMG system [48, 49]. In addition, m decreases slightly upon addition of Er as the addition of rare-earth in Zr-based BMGs usually results in the improvement of glass-forming ability, which is believed as the characteristic of strong liquid [33, 34, 45, 50]. On the other hand, it is not appropriate to explain the better formability of Zr65Er2 from the perspective of fragility index.

4. Discussion

Wide SCLR and large fragility are generally considered as the main reasons for better formability, while the effect of T_g on formability has not received much attention. The contribution of T_g to formability can be simply explained based on the feature of Angell plot as described in this paper. In Angell plot, the SCLR of most BMGs with an intermediate to strong liquid behavior and a relative narrow width ($0.85 < T_g/T_x < 1$), can be simplified to be linear with the slope of m, which is contrast to the obviously curving SCLR of the very fragile liquid [51], as shown in Fig. 7. This linear simplification can be applied for Zr65 and Zr65Er2 since they have obviously strong liquid feature with small m and their T_g/T_x are 0.846 and 0.835 respectively. By using the linear simplification, the viscosity drop in the whole SCLR, which is also an indicator of the formability [17], can be estimated as:

$$(\mathrm{Log}_{10}\,\eta_{T_g} - \mathrm{Log}_{10}\,\eta_{T_x}) \approx m \times (1 - \frac{T_g}{T_x}) = \frac{m \times \Delta T_x}{T_g + \Delta T_x} \qquad (4).$$
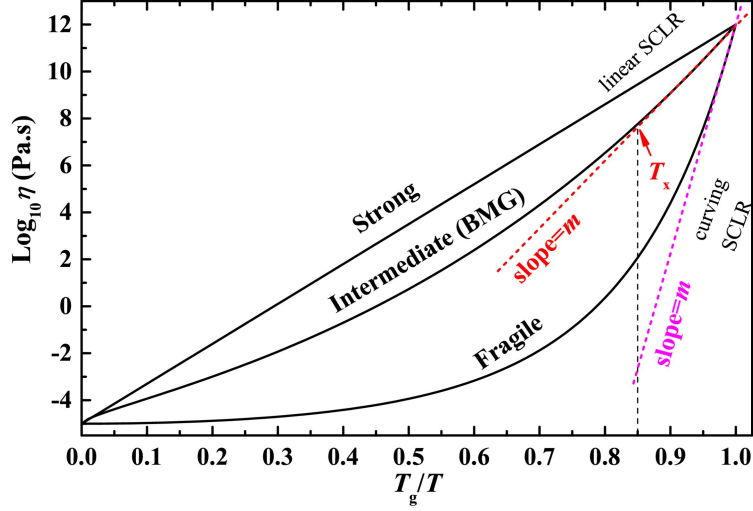
Fig. 7 Linear simplification of SCLR in Angell plot.

From Eq. (4), a BMG with a significantly lower T_g has thus a better formability even though it does not have the obviously large m and ΔT_x. To name a few of this type of BMGs, $Mg_{65}Cu_{25}Y_{10}$ (T_g=155 °C) [25], $Au_{49}Ag_{5.5}Pd_{2.3}Cu_{26.9}Si_{16.3}$ (T_g=130 °C) [26] and $Ce_{70}Al_{10}Cu_{20}$ (T_g=68 °C) [27] are some of them. The last one is labeled as the so-called "amorphous metallic plastic" as it can be imprinted by hand in nearly-boiling water. For more BMGs with a wide distribution of T_g, ΔT_x and m, there is still a considerable correlation between T_g and formability. Such as 18 Be-free Zr-based BMGs [16] and 10 Zr-, Pd-, Pt-, Au-, Mg-, Fe-based BMGs [18]. For the two BMGs investigated in this research, by putting the values of T_g, ΔT_x and m into Eq. (4), the $(\mathrm{Log}_{10}\eta_{T_g} - \mathrm{Log}_{10}\eta_{T_x})$ of Zr65 and Zr65Er2 is calculated as 3.2 and 3.3, respectively. This is in a good agreement with the experimental $\Delta(\mathrm{Log}_{10}\eta)$ value of 3.5 for Zr65 and 3.7 for Zr65Er2. Therefore, addition to the larger ΔT_x, the lower T_g has also important contribution to the better formability of Zr65Er2 than that of Zr65.

Except T_g, other transition temperatures, including T_x, T_m and T_l also decrease after addition of Er, as listed in Table 1. This synchronous decrease in the transition temperatures is a common

phenomenon when adding minor heavy rare earth elements into Zr-based and Cu-Zr based BMGs to achieve better glass-forming ability, such as addition of Gd, Ho and Y into $(CuZr)_{93}Al_7$ [52], Y and Er into $Zr_{50}Cu_{30}Ni_5Al_{10}$ [53], Gd, Y, Dy and Lu into $Cu_{47}Zr_{45}Al_8$ [54], Dy, Gd and Er into $Zr_{62.5}Cu_{22.5}Fe_5Al_{10}$ [55], Gd into $Zr_{46}Cu_{46}Al_8$ [37], $Zr_{48}Cu_{45}Al_7$ [56], $Zr_{52.2}Cu_{39.1}Al_{8.7}$ [57] and $Cu_{50}Zr_{42}Al_8$ [58], Y into $Zr_{55}Cu_{20}Ni_{10}Al_{15}$ [59], $Zr_{58}Nb_3Cu_{16}Ni_{13}Al_{10}$ [60] and $Zr_{50}Cu_{25}Ni_{10}Al_{15}$ [61], etc. Another notable common feature in the above cases is that the lower melting point after addition of rare-earth is not caused by the composition shift to eutectic [37, 54-60], although the deep eutectic composition usually has a lower melting point and a better glass-forming ability [62]. This is also the case for Zr65Zr2, as shown in Fig. 4. Both Zr65 and Zr65Er2 have obviously off-eutectic feature and the later has a more endothermic peak.

The atom radius of most heavy rare earth elements is 0.17-0.18 nm (0.17558 nm for Er), larger than those of Zr (0.16025 nm), Cu (0.12780 nm), Ni (0.12459 nm) and Al (0.14317 nm). Minor addition of rare-earth atom increases the constituent atoms space misfit and favors the formation of short-range ordering with a closer packed local structure. In addition, the heat of mixing of Cu-Er, Ni-Er and Al-Er are -23, -34 and -38 KJ/mol respectively. The large negative heat of mixing enhances interaction among the components and also favors the formation of short-rang ordering. Compared with the long-range ordering, the atom redistribution of the short-range ordering is easier and needs lower energy and thus lower temperature in the thermal excited transitions, including glass transition, crystallization and melting. The extra endothermic peak of Zr65Er2 is very likely related to the melting of some phases evolved from the short-range ordering. Based on the above explanation, the lower T_g, T_x, T_m and T_l

after minor addition of rare-earth is mostly attributed to the formation of short-range ordering with lower transition energy rather than composition shift to near eutectic.

5. Conclusions

The softness of Zr65Er2 is 43% larger than that of Zr65, which makes Zr65Er2 to be a very formable Be-free Zr-based BMG. Except the lager ΔT_x, the obviously lower T_g has the most significant contribution to the improvement of formability. This phenomenon is well explained by the linear SCLR simplification in Angell plot. In addition, the addition of large Er atom is believed to favors the formation of short-range ordering with lower transition energy, resulting in the lower transition temperatures including T_g, T_x, T_m and T_l. These findings help understand the effect of minor addition of rare-earth to the formability of Zr-based bulk metallic glasses, and provide an effective way to further develop new Be-free Zr-based BMGs with better formability comparable to the Be-added Zr-based BMGs and noble-metal-based BMGs.

References

[1] M.d. Oliveira, W.J.B. F, A.R. Yavari. *Mater Trans JIM* 2000;41:1501.

[2] A.R. Yavari, M.F.d. Oliveira, W.J. Botta. *MRS Proceedings* 2000;644:20.

[3] Y. Saotome, S. Miwa, T. Zhang, A. Inoue. *J Mater Process Tech* 2001;113:64.

[4] Y. Saotome, Y. Noguchi, T. Zhang, A. Inoue. *Materials Science and Engineering: A* 2004;375-377:389.

[5] J. Schroers. *Adv Mater* 2010;22:1566.

[6] G. Kaltenboeck, T. Harris, K. Sun, T. Tran, G. Chang, J.P. Schramm, M.D. Demetriou, W.L. Johnson. *Sci. Rep.* 2014;4:6441.

[7] L. Liu, M. Hasan, G. Kumar. *Nanoscale* 2014;6:2027.

[8] J. Qiang, D. Estevez, Y. Dong, Q. Man, C. Chang, X. Wang, R.-W. Li. *J Appl Phys* 2014;116:093911.

[9] N. Yodoshi, R. Yamada, A. Kawasaki, A. Makino. *J Alloy Compd* 2014;615:S61.

[10] Z. Hu, S. Gorumlu, B. Aksak, G. Kumar. *Scripta Mater* 2015;108:15.

[11] M. Kanik, P. Bordeenithikasem, D. Kim, N. Selden, A. Desai, R. M'Closkey, J. Schroers. *J Microelectromech S* 2015;24:19.

[12] P. Vella, S. Dimov, E. Brousseau, B. Whiteside. *Int. J. Aav. Manuf. Tech.* 2015;76:523.

[13] J. Ma, X. Liang, X. Wu, Z. Liu, F. Gong. *Sci. Rep.* 2015;5:17844.

[14] E.B. Pitt, G. Kumar, J. Schroers. *J Appl Phys* 2011;110:043518.

[15] T.G. Nieh, J. Wadsworth, C.T. Liu, T. Ohkubo, Y. Hirotsu. *Acta Mater* 2001;49:2887.

[16] J. Schroers. *Acta Mater* 2008;56:471.

[17] H. Kato, T. Wada, M. Hasegawa, J. Saida, A. Inoue, H.S. Chen. *Scripta Mater*

2006;54:2023.

[18]Q. Hu, M.W. Fu, X.R. Zeng. *J Alloy Compd* 2014;602:326.

[19]Q. Hu, M.W. Fu, X.R. Zeng. *Mater Design* 2014;64:301.

[20]S. Ding, Y. Liu, Y. Li, Z. Liu, S. Sohn, F.J. Walker, J. Schroers. *Nat Mater* 2014;13:494.

[21]C.A. Angell. *Science* 1995;267:1924.

[22]Z.P. Lu, C.T. Liu. *Acta Mater* 2002;50:3501.

[23]H.J. Willy, L.Z. Zhao, G. Wang, Z.W. Liu. *Physica B: Condens Matter* 2014;437:17.

[24]J. Schroers, G. Kumar, T.M. Hodges, S. Chan, T.R. Kyriakides. *JOM* 2009;61:21.

[25]B. Gun, K.J. Laws, M. Ferry. *J Non-cryst Solids* 2006;352:3896.

[26]J. Schroers, B. Lohwongwatana, W.L. Johnson, A. Peker. *Mater Sci Eng A* 2007;449-451:235.

[27]B. Zhang, D.Q. Zhao, M. Pan, R.J. Wang, W.H. Wang. *Acta Mater* 2006;54:3025.

[28]Q. Luo, W.H. Wang. *J Non-cryst Solids* 2009;355:759.

[29]S. Cardinal, J. Qiao, J.M. Pelletier, H. Kato. *Intermetallics* 2015;63:73.

[30]W. Zhang, H. Guo, Y. Li, Y. Wang, H. Wang, M. Chen, S. Yamaura. *J Alloy Compd* 2014;617:310.

[31]D. Wang, G. Liao, J. Pan, Z. Tang, P. Peng, L. Liu, T. Shi. *J Alloy Compd* 2009;484:118.

[32]D.V. Louzguine-Luzgin, T. Wada, H. Kato, J. Perepezko, A. Inoue. *Intermetallics* 2010;18:1235.

[33]W.H. Wang. *Prog Mater Sci* 2007;52:540.

[34]Z.P. Lu, C.T. Liu. *J Mater Sci* 2004;39:3965.

[35]M.J. Stefan. *Akad Wiss Wien Math-Nat Klasse Abt 2* 1874;69:713.

[36] D. Suh, R. Dauskardt. *J Mater Res* 2002;17:1254.

[37] P. Yu, H.Y. Bai, W.H. Wang. *J Mater Res* 2006;21:1674.

[38] R. Bruning, K. Samwer. *Phys Rev B* 1992;46:11318.

[39] Z.F. Zhao, Z. Zhang, P. Wen, M.X. Pan, D.Q. Zhao, W.H. Wang, W.L. Wang. *Appl Phys Lett* 2003;82:4699.

[40] L. Shadowspeaker, R. Busch. *Appl Phys Lett* 2004;85:2508.

[41] B. Zhang, R.J. Wang, D.Q. Zhao, M.X. Pan, W.H. Wang. *Phys Rev B* 2004;70:224208.

[42] L. Hu, F. Ye, Y.F. Liang, J.P. Lin. *Appl Phys Lett* 2012;100:021906.

[43] J.H. Na, M.D. Demetriou, W.L. Johnson. *Appl Phys Lett* 2011;99:161902.

[44] E.S. Park, J.H. Na, D.H. Kim. *Appl Phys Lett* 2007;91:031907.

[45] O.N. Senkov. *Phys Rev B* 2007;76:104202.

[46] C. Zhang, L. Hu, Y. Yue, J.C. Mauro. *J Chem Phys* 2010;133:014508.

[47] Y. Zhao, X. Bian, K. Yin, J. Zhou, J. Zhang, X. Hou. *Physica B: Condens Matter* 2004;349:327.

[48] W.K. An, X. Xiong, Y. Liu, A.H. Cai, G.J. Zhou, Y. Luo, T.L. Li, X.S. Li. *Trans Nonferrous Met Soc China* 2013;23:3312.

[49] Y.H. Liu, G. Wang, R.J. Wang, D.Q. Zhao, M.X. Pan, W.H. Wang. *Science* 2007;315:1385.

[50] R. Busch, J. Schroers, W.H. Wang. *Mrs Bull* 2007;32:620.

[51] D. Louzguine-Luzgin, N. Chen, A. Churymov, L. Louzguina-Luzgina, V. Polkin, L. Battezzati, A. Yavari. *J Mater Sci* 2015;50:1783.

[52] B. Huang, H.Y. Bai, W.H. Wang. *J Appl Phys* 2011;110:123522.

[53] J. Luo, H.P. Duan, C.L. Ma, S.J. Pang, T. Zhang. *Mater Trans* 2006;47:450.

[54] L. Deng, B.W. Zhou, H.S. Yang, X. Jiang, B.Y. Jiang, X.G. Zhang. *J Alloy Compd* 2015;632:429.

[55] A.Y. Churyumov, A.I. Bazlov, A.A. Tsarkov, A.N. Solonin, D.V. Louzguine-Luzgin. *J Alloy Compd* 2016;654:87.

[56] X. Xu, L.Y. Chen, G.Q. Zhang, N. Wang, J.Z. Jiang. *Intermetallics* 2007;15:1066.

[57] Y. Xu, Y. Wang, X. Liu, G. Chen, Y. Zhang. *J Mater Sci* 2009;44:3861.

[58] L. Zhang, D. Luo, S. Kou. *Rare Metal Mat Eng* 2012;41:1903.

[59] Y. Zhang, M. Pan, D. Zhao, R. Wang, W. Wang. *Mater Trans JIM* 2000;41:1410.

[60] X. Zhao, C. Ma, S. Pang, T. Zhang. *Phil Mag Lett* 2009;89:11.

[61] W. Long, X. Ouyang, Z. Luo, J. Li, A. Lu. *Physica B: Condens Matter* 2011;406:503.

[62] Y. Li. *Mater Trans JIM* 2001;42:556.